Full Paper

CSIRO PUBLISHING

Aust. J. Chem. **2010**, *63*, 1334–1341

www.publish.csiro.au/journals/ajc

Tuning Coordination Environments Through Ligand Redox Chemistry: the Thiol–Disulfide Reaction

Edwin C. Constable,[A] *Catherine E. Housecroft,*[A,B] *Markus Neuburger,*[A] *Jason R. Price,*[A] *and Jennifer A. Zampese*[A]

[A]Department of Chemistry, University of Basel, Spitalstrasse 51, CH–4056 Basel, Switzerland.
[B]Corresponding author. Email: catherine.housecroft@unibas.ch

Oxidative coupling of 6-(pyridin-2-yl)pyridine-2(1*H*)-thione yields 1,2-bis(2,2′-bipyridin-6-yl)disulfide (**4**), which can act as a bis(chelate) to a single zinc(II) centre. The effects on the solid-state structure of introducing a methyl substituent into each 6-position of **4** have been examined. Ligand **4** functions as a bridging ligand in $[Cu_2(\mu\text{-}\mathbf{4})(\mu\text{-}\mathbf{6})]^{4+}$ in which ligand **6** is 1,2-bis(2,2′:6′,2″-terpyridin-4′-yl)disulfide; $[Cu_2(\mu\text{-}\mathbf{4})(\mu\text{-}\mathbf{6})]^{4+}$ self-assembles from the components according to the preference shown by copper(II) for a five-coordinate {Cu(bpy)(tpy)} environment. Reaction of **4** with $[Cu(NCMe)_4][PF_6]$ leads to a product, tentatively formulated as $\{[Cu(\mathbf{4})][PF_6]\}_n$, which, in air, undergoes oxidation of both copper and ligand to yield $[Cu(\mathbf{5})_2]$ (H**5** = 2,2′-bipyridine-6-sulfonic acid), the solid state structure of which is presented.

Manuscript received: 3 March 2010.
Manuscript accepted: 19 May 2010.

Introduction

We have recently become interested in the development of self-replicating systems based on coordination chemistry. The basis of our approach is three-fold: (i) the preference of copper(II) centres for five-coordinate tpy-bpy environments; (ii) the oxidation of thiols to disulfides by copper(II) with concomitant reduction to copper(I); and (iii) the preference of copper(I) for four-coordinate bpy-bpy environments.[1–3] This has led us to investigate fundamental aspects of the interactions of thiol ligands with copper species, and in this paper, we report studies on oligopyridine thiols (thiones) and disulfides. It is well established that pyridinethiols show a strong preference for the thione tautomeric form both in the solid state and in polar solvents.[4–7] Although 1,10-phenanthrolinethiols (thiones)[8–10] are well known, thiol (thione) derivatives of 2,2′-bipyridine[3,11–14] and 2,2′:6′,2″-terpyridine[15,16] have received relatively little attention. Of significant interest is the facile oxidative coupling of thiols to disulfides (Eqn 1). Thiol(thione)–disulfide interconversion (Eqn 1) has been used to establish dynamic combinatorial libraries,[17–19] and several recent reports have appeared concerning the in situ formation of dipyridyl disulfides and their incorporation into coordination complexes.[20–23]

$$2\mathrm{RSH} \rightarrow \mathrm{RSSR} + 2\mathrm{H}^+ + 2\mathrm{e}^- \qquad (1)$$

We have recently shown that the conversion of 6-(6-methylpyridin-2-yl)pyridine-2(1*H*)-thione (**1**, Scheme 1) to 1,2-bis(6′-methyl-2,2′-bipyridin-6-yl)disulfide (**2**, Scheme 2) changes the metal-binding domain from a monodentate *S*-donor to an *N*,*N*′-chelate,[3] and we illustrated this phenomenon within a series of copper(I) complexes, the stabilization of which required the incorporation of the methyl substituent.[24] We now report the oxidative coupling of 6-(pyridin-2-yl)pyridine-2(1*H*)-thione (**3**) to 1,2-bis(2,2′-bipyridin-6-yl)disulfide (**4**), in which the flexible disulfide backbone permits the ligand to bind a single metal ion in a bis(chelate) mode, or to act as a bridging ligand. Although compound **3** has been previously reported,[13,14,17] the oxidative coupling to **4** and the coordination chemistry of this attractive ligand remain unexplored.

Results and Discussion

The yellow thione **3** was prepared by treating 6-chloro-2,2′-bipyridine[25] with $NaSH{\cdot}xH_2O$ in DMF followed by workup under aqueous conditions at pH 7. The ^1H and ^{13}C NMR spectra[14] were acquired in the presence of dithiothreitol to prevent oxidative coupling of the thione,[26] and have been reassigned[14] using NOESY, COSY, HMQC, and HMBC techniques. The broadened signal assigned to H^{A6} (see Scheme 1) is indicative of hindered rotation of the 2,2′-bipyridine (bpy) unit, and is consistent with the presence of an NH···N hydrogen bond in the thione tautomer. Recrystallization of **3** from Et_2O gave X-ray-quality crystals and structural analysis confirmed the thione form of the compound (Fig. 1). The bpy unit in each of the two independent molecules of **3** is in a *cis*-conformation constrained by the NH···N hydrogen bond, and is planar; the angles between the least-squares planes of the two pyridine rings in the two molecules are 5.11(9) and 1.87(8)°. In the solid-state structure of compound **1**, we observed that face-to-face π-interactions between pyridine-2(1*H*)-thione rings were a primary feature of the packing, although the steric demands of the methyl substituents precluded π-stacking of the methylpyridine rings. In **3**, the packing is best described in terms of stacked sheets. Each sheet assembles through short S···H contact between pairs of independent molecules (S1···H131C13 = 2.98, S1···C13 = 3.8645(18) Å, S1···H131–C13 = 156°) and non-classical CH···N hydrogen bonds (C12H121···N2 = 2.77, C12···N2 = 3.713(2) Å, C12–H121···N2 = 180°; C2H21···N4^i = 2.71, C2···N4^i = 3.641(2) Å, C2–H21···N4^i = 173°, symmetry code i = −1 + *x*,

10.1071/CH10105 0004-9425/10/091334

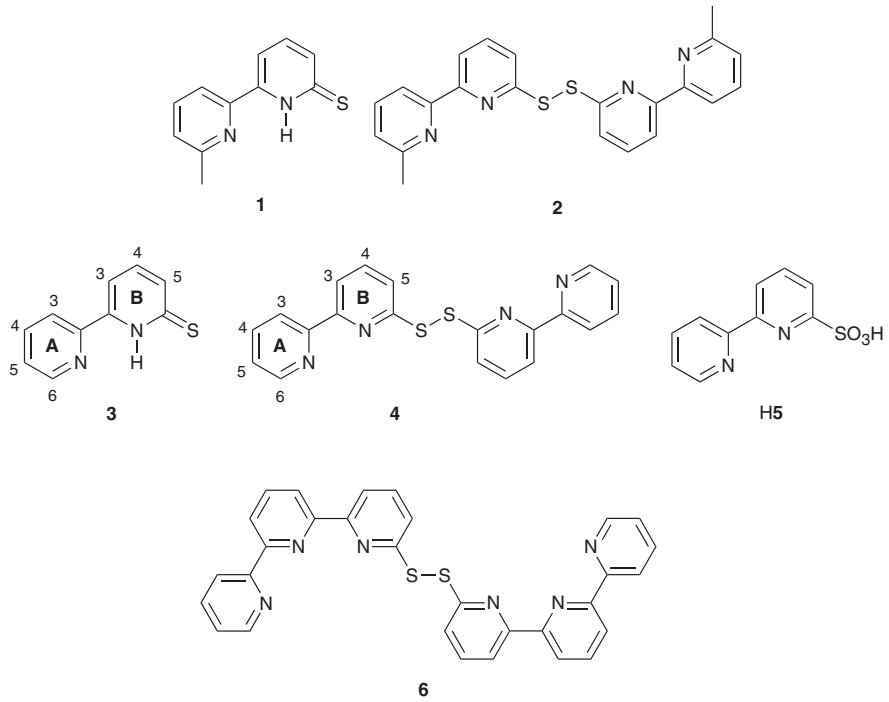

Scheme 1. Ligand structures and atom labelling for NMR spectroscopic assignments.

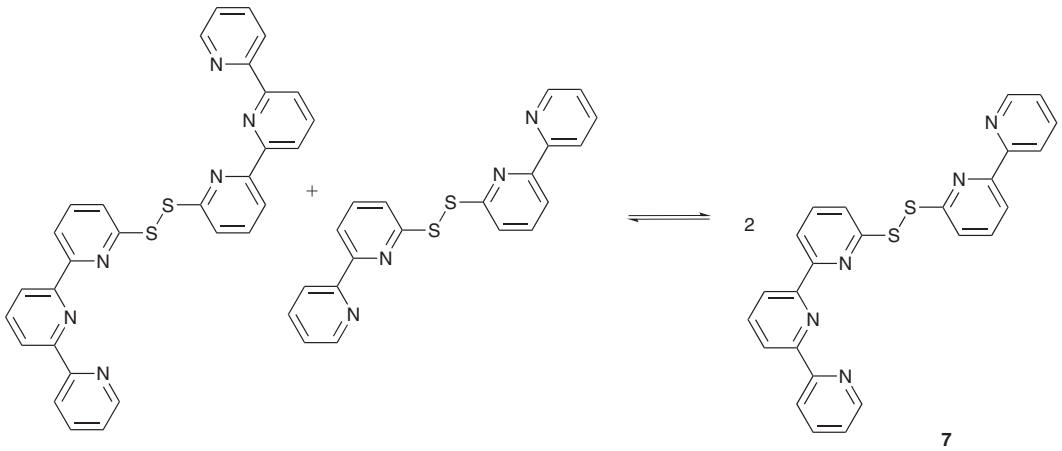

Scheme 2. Proposed formation of ligand **7** in the electrospray mass spectrometer.

$-1+y$, z). The packing of the sheets is such that adjacent molecules are arranged in centrosymmetric pairs (shown on the left of Fig. 2b for molecules containing atom S2) or in pairs in which the molecules are orthogonal to one another (Fig. 2b, right). The distances between sheets are consistent with π-stacking pervading the structure.

When solutions of **3** are left in air, the thione oxidizes to **4**. The reaction can be carried out preparatively by treating a MeCN solution of **3** with H_2O_2. In the electrospray mass spectrum of **4**, peaks at *m/z* 397.3 and 375.3 were assigned to $[M+Na]^+$ and $[M+H]^+$; the isotope distributions matched those simulated. The ^1H and ^{13}C NMR spectra of a $CDCl_3$ solution of **4** were assigned by 2D-techniques. In the ^{13}C NMR spectrum, the most diagnostic feature of the spectrum is the change in chemical shift for the sulfur-attached carbon atom, C^{B6}, from δ 179.5 ppm in **3** to 158.6 ppm in **4**. In the ^1H NMR spectrum, the signal for H^{B3} (the proton *para* to the position of sulfur attachment) is significantly affected by the thione to disulfide transformation, shifting from δ 7.18 to 8.20 ppm on going from **3** to **4**. With the exception of the appearance of a resonance for proton H^{A6} (Scheme 1), the pattern of signals in the ^1H NMR spectrum of **4** is similar to that in **2**. Single crystals of **4** were selected from the bulk sample, and Fig. 3 depicts the molecular structure. One of the interesting features of ligands containing polysulfide bridges is the helical twist that renders the ligand chiral in the solid state. Compound **4** crystallizes in the centrosymmetric space group *C*2/*c* with both the *P* and *M* forms present. There is one independent half-molecule in the asymmetric unit, and the bpy domain is close to planar (angle between the least-squares planes of the two pyridine rings is 11.22(6)°). It adopts a *trans*-conformation, and the switch from *cis* to *trans* on going from **3** to **4** is consistent with the loss of the NH···N hydrogen bond. The angle between the least-squares planes of the sulfur-bonded pyridine rings of 76.3° is smaller than the 88.8° observed in the

methyl derivative **2**,[3] and this is most likely associated with the differences in packing between the two compounds. A principal packing motif in both **2** and **4** is a centrosymmetric pair of molecules that associate through face-to-face π-stacking of bpy units. In **2**, the methyl substituents prevent efficient stacking of these domains throughout the lattice.[3] However, in **4**, the face-to-face interactions at separations of 3.5 Å between molecules of alternating *P* and *M* chirality generate infinite chains (Fig. 4a). The latter are aligned in the same direction through the lattice (Fig. 4b), and intermolecular interactions between adjacent chains are predominantly CH···S (S1···H10A^{ii} = 2.94 Å, symmetry code ii = ½ + *x*, −½ + *y*, *z*) and CH···N contacts (N2···H8A^{iii} = 2.73, N1···H4A^{iv} = 2.72 Å, symmetry codes iii = *x*, 2 − *y*, ½ + *z*, iv = ½ − *x*, −½ + *y*, ½ − *z*). The overall packing efficiencies of **4** and **2** are 71.3 and 69.3% respectively.

We have previously illustrated the ability of **2** and its trisulfide analogue to coordinate to copper(I) through the bpy binding domains and to adopt bridging modes between two copper(I) centres.[3] We decided to initiate our investigations of the metal-binding properties of **4** by comparing the reactions of zinc(II) with **2** and **4**. Acetonitrile solutions of **2** or **4** were treated with $Zn(ClO_4)_2 \cdot 6H_2O$ under reflux. The products were isolated as colourless crystalline solids after diffusion of Et_2O into the reaction mixtures. Elemental analysis of each product indicated a 1:1 ratio of Zn:ligand, and dominant peak envelopes in the matrix-assisted laser desorpton–ionization (MALDI) mass spectra at *m/z* 466.53 and 538.57 respectively were assigned to the ions $[Zn(\mathbf{2})]^+$ and $[Zn(\mathbf{4})ClO_4]^+$. The base peak, however, in each spectrum was consistent with loss of sulfur from each ligand and appeared at *m/z* 370.52 (derived from **2**) and at *m/z* 342.52 (derived from **4**). All the observed isotope distributions matched those simulated. The elemental and mass spectrometric analyses therefore suggested the formation of $[Zn(L)][ClO_4]_2$ where L = **2** or **4**. Attempts to obtain an electrospray mass spectrum of the complex containing ligand **2** yielded peaks assigned to $[\mathbf{2} + H]^+$ (*m/z* 403.2, base peak) and $[\mathbf{2} + Na]^+$ (*m/z* 425.1), but no zinc-containing ions were observed.

When compared with the ^{1}H NMR spectra of the free ligands **2**[3] and **4**, the spectra of the complexes showed a characteristic pattern in values of $\Delta\delta$ [$\Delta\delta = \delta_{complex}(CD_3CN) - \delta_{ligand}(CDCl_3)$]. The signal for H^{A6} in **4** shifted to lower frequency on complex formation ($\Delta\delta = -0.27$). All other signals shifted to higher frequency, the largest values of $\Delta\delta$ being for H^{A4} ($\Delta\delta = +0.68$ for **2**, and +0.69 for **4**) and H^{B4} ($\Delta\delta = +0.68$ for **2**, and +0.60 for **4**).

Single crystals of $2\{[Zn(\mathbf{2})(OClO_3)][ClO_4]\} \cdot EtOH$ and $[Zn(\mathbf{4})(OClO_3)][ClO_4]$ were grown by slow diffusion of Et_2O into an EtOH solution of $[Zn(\mathbf{2})][ClO_4]_2$ and into an MeCN solution of $[Zn(\mathbf{4})][ClO_4]_2$ respectively. In both compounds, one perchlorate ion is coordinated to the zinc(II) ion (Figs 5 and 6a). $[Zn(\mathbf{4})(OClO_3)][ClO_4]$ contains two independent formula units in the asymmetric unit. The description of the structures as five- rather than six-coordinate zinc(II) has been made by

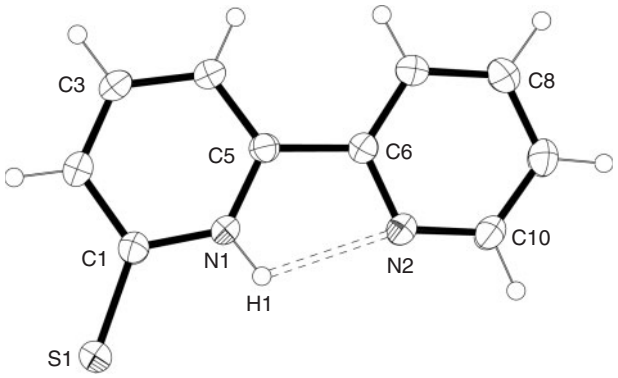

Fig. 1. Structure of one of the two independent molecules of **3** (ellipsoids plotted at 40% probability level). Selected bond parameters: S1–C1 = 1.6749(18), N1–C1 = 1.368(2), N1–C5 = 1.357(2), N2–C6 = 1.347(2), N2–C10 = 1.337(2), C1–C2 = 1.418(2), C2–C3 = 1.359(2), C3–C4 = 1.399(2), C4–C5 = 1.373(2), C5–C6 = 1.475(2), C6–C7 = 1.381(2), C7–C8 = 1.378(3), C8–C9 = 1.378(3), C9–C10 = 1.386(3) Å; S1–C1–C2 = 125.65(14), N1–C1–S1 = 120.16(12)°. Parameters for the second molecule are similar.

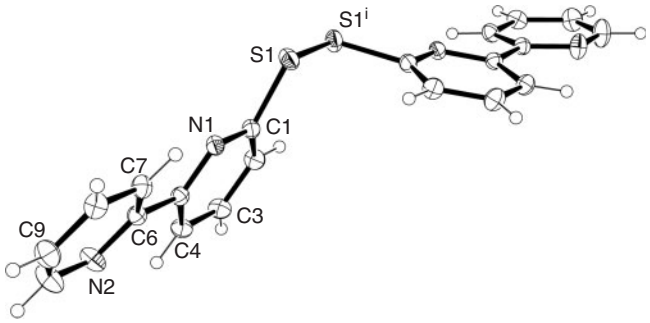

Fig. 3. Molecular structure of **4** (ellipsoids plotted at 40% probability level); symmetry code i = 1 − *x*, *y*, ½ − *z*. Important bond parameters: S1–C1 = 1.7806(11), S1–S1^i = 2.0198(9) Å; C1–S1–S1^i = 106.41(4)°; torsion angle C1–S1–S1^i–C1^i = −99.12(6)°.

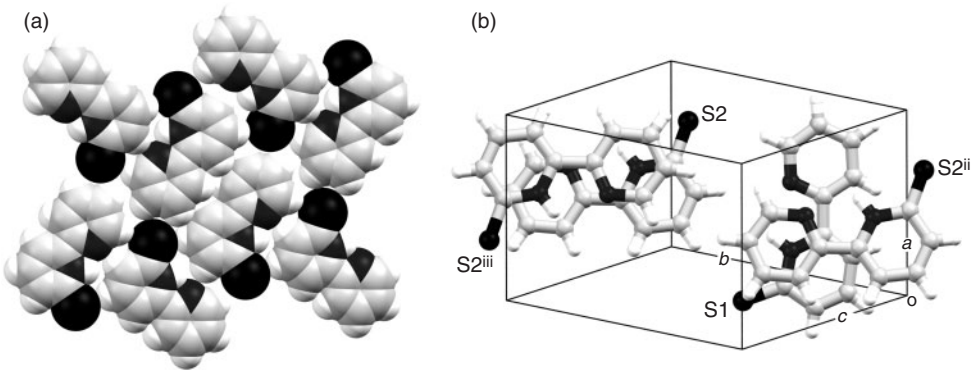

Fig. 2. Packing of molecules of **1**: (a) assembly of sheets, and (b) stacking motifs between sheets. Symmetry codes ii = *x*, −1 + *y*, *z*, iii = 1 − *x*, 2 − *y*, 1 − *z*.

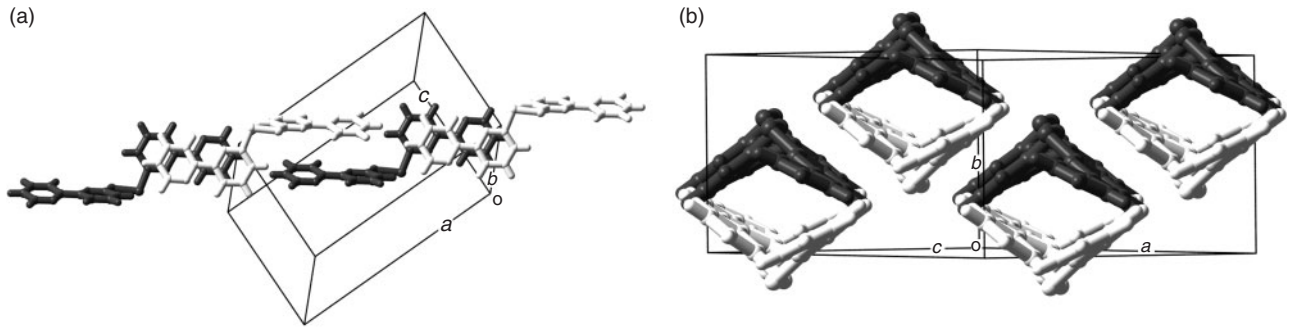

Fig. 4. Packing of molecules of **4**: (a) face-to-face bpy···bpy interactions between molecules of alternating *P* and *M* chirality produce chains, and (b) alignment of chains through the lattice.

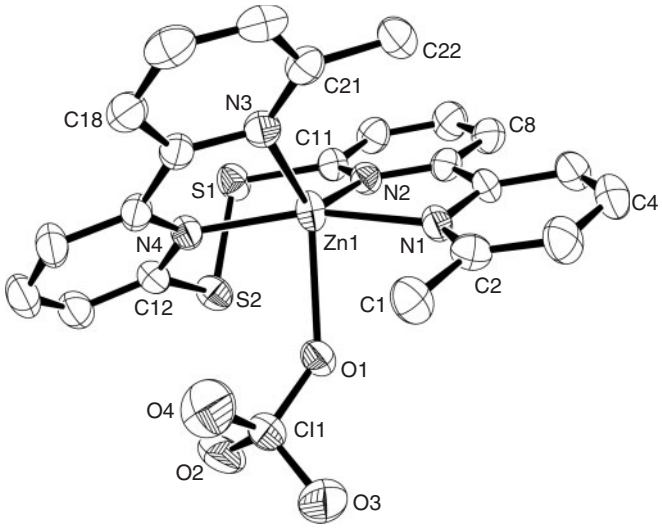

Fig. 5. Structure of the $[Zn(\mathbf{2})(OClO_3)]^+$ cation in $2\{[Zn(\mathbf{2})(OClO_3)][ClO_4]\}\cdot EtOH$ (ellipsoids plotted at 40% probability level); H atoms are omitted. Selected bond parameters: Zn1–N1 = 2.064(5), Zn1–N2 = 2.051(5), Zn1–N3 = 2.138(5), Zn1–N4 = 2.018(5), Zn1–O1 = 2.324(4), S1–S2 = 2.042(2) Å; N1–Zn1–N2 = 81.81(18), N1–Zn1–N3 = 98.93(18), N2–Zn1–N3 = 128.99(18), N1–Zn1–N4 = 160.52(19), N2–Zn1–N4 = 114.18(18), N3–Zn1–N4 = 79.94(18), N1–Zn1–O1 = 81.32(16), N2–Zn1–O1 = 106.52(16), N3–Zn1–O1 = 124.13(16), N4–Zn1–O1 = 83.32(16), Zn1–O1–Cl1 = 139.7(2), C11–S1–S2 = 104.0(2), C12–S2–S1 = 100.6(2)°.

comparing the sum of the Shannon ionic radii[27] with the observed Zn···O contact distances to the second perchlorate anion (3.639(10) Å in $2\{[Zn(\mathbf{2})(OClO_3)][ClO_4]\}\cdot EtOH$; 2.6232(15) and 3.0039(19) Å for the two independent cations in $[Zn(\mathbf{4})(OClO_3)][ClO_4]$). In each structure, the disulfide ligand acts as a bis(chelate), coordinating to the zinc(II) ion through the four nitrogen donors. Each of the $[Zn(\mathbf{2})(OClO_3)]^+$ and $[Zn(\mathbf{4})(OClO_3)]^+$ cations is chiral, and both *P* and *M* forms are present in the crystal lattice of each complex. The pitch of the helix (Fig. 6b) in each complex can be defined by the angle between the least-squares planes through the two chelate rings. In $[Zn(\mathbf{2})(OClO_3)]^+$, this angle is 51.3(5)°, and in the two independent $[Zn(\mathbf{4})(OClO_3)]^+$ cations, the corresponding angles are 35.59(12) and 37.27(12)°. The change on going from $[Zn(\mathbf{2})(OClO_3)]^+$ to $[Zn(\mathbf{4})(OClO_3)]^+$ is attributed to the steric repulsion between the two methyl substituents in the former. In $2\{[Zn(\mathbf{2})(OClO_3)][ClO_4]\}\cdot EtOH$, centrosymmetric pairs of cations engage in face-to-face π-stacking of the bpy units containing atoms N1 and N2 at a separation of 3.59 Å. The additional, dominant packing forces involve extensive $CH_{pyridine}\cdots O_{perchlorate}$ and $OH_{EtOH}\cdots S$ short contacts. The ethanol molecule is disordered and has been modelled over two sites related by a two-fold axis. Crystal packing motifs in $[Zn(\mathbf{4})(OClO_3)][ClO_4]$ resemble those in $2\{[Zn(\mathbf{2})(OClO_3)][ClO_4]\}\cdot EtOH$. One bpy domain in each independent $[Zn(\mathbf{4})(OClO_3)]^+$ forms a π-stack across an inversion centre to an adjacent cation (separations are 3.44 Å for $N1/N2\cdots N1^{i}/N^{i}$ and 3.63 Å for $N7/N8\cdots N7^{ii}/N8^{ii}$; symmetry codes i = 2 − *x*, 2 − *y*, 1 − *z*, ii = 1 − *x*, 1 − *y*, 1 − *z*). Extensive $CH_{pyridine}\cdots O_{perchlorate}$ interactions make a dominant contribution to the overall packing.

The manner in which ligands **2** and **4** envelop a zinc(II) ion contrasts with the bridging mode that we have previously observed for **2** and its trisulfide analogue when they are bound to copper(I).[3] Despite the fact that the $\{Cu(bpy)_2\}^+$ coordination sphere usually requires the presence of substituents in 6′- or 6,6′-positions to stabilize copper(I),[28] we decided to investigate the coordination of ligand **4** to copper(I). The reaction of **4** with $[Cu(NCMe)_4][PF_6]$ in MeCN led, after workup, to a red-orange solid. The ^1H NMR spectrum of a CD_3CN solution of the compound exhibited seven broadened resonances between δ 8.5 and 7.5 ppm, consistent with diamagnetic copper(I) and the presence of **4** in a symmetrical environment. However, we cannot rule out the presence of the coordinated thione **3**. All attempts to isolate a pure sample of the product were unsuccessful. It is significant that when $[Cu(NCMe)_4][PF_6]$ reacts with ligand **2**, a similarly broadened ^1H NMR spectrum is obtained and in this case, we tentatively proposed the formation of $\{[Cu(\mathbf{2})][PF_6]\}_n$.[3] By analogy, we propose the formation of $\{[Cu(\mathbf{4})][PF_6]\}_n$.

The product of the reaction of $[Cu(NCMe)_4][PF_6]$ and **4** was left to stand in the NMR tube for several months, after which time X-ray-quality green crystals had grown. Structural analysis revealed the formation of $[Cu(\mathbf{5})_2]\cdot 2.5MeCN$ containing an unusual sulfonate ligand, confirming the aerial oxidation of both the metal and ligand (see Scheme 1 for the structure of H**5**). The structure of $[Cu(\mathbf{5})_2]$ is presented in Fig. 7. The oxidative cleavage of ligand **4** is similar to that observed by Delgado et al. during the reaction of 1,2-di(pyridin-2-yl)disulfide with copper(II) nitrate. In this case, however, the conjugate bases of both pyridine-2-sulfonic acid and pyridine-2-sulfinic acid were produced.[29] The copper(II) centre in $[Cu(\mathbf{5})_2]$ is in an octahedral environment with the two *N*,*N*′,*O*-donors adopting a *mer*-arrangement. The chiral complex crystallizes in the *P*−1 space group with both enantiomers in the unit cell. This pair of enantiomers associates through face-to-face stacking of bpy

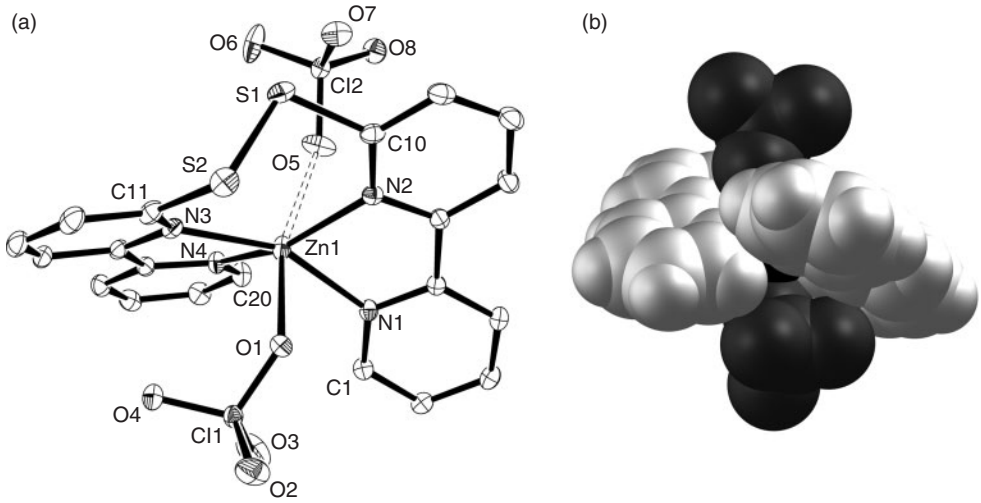

Fig. 6. (a) Structure of one of the independent $[Zn(\mathbf{4})(OClO_4)]^+$ cations in $[Zn(\mathbf{4})(OClO_4)][ClO_4]$ showing close contact to the second perchlorate ion; ellipsoids plotted at 40% probability level and H atoms are omitted. Selected bond parameters: Zn1–N1 = 2.1082(14), Zn1–N2 = 2.0592(14), Zn1–N3 = 2.1140(14), Zn1–N4 = 2.0764(14), Zn1–O1 = 2.3059(13), Zn1–O5 = 2.6232(15), S1–S2 = 2.0388(7) Å; N1–Zn1–N2 = 80.07(5), N1–Zn1–N3 = 156.68(5), N2–Znl–N3 = 116.90(5), N1–Zn1–N4 = 94.16(5), N2–Zn1–N4 = 150.26(5), N3–Zn1–N4 = 78.54(5), N1–Zn1–O1 = 82.43(5), N2–Zn1–O1 = 91.36(5), N3–Zn1–O1 = 81.35(5), N4–Zn1–O1 = 116.97(5), O1–Zn1–O5 = 164.59(5)°. For the second independent $[Zn(\mathbf{4})(OClO_4)]^+$ cation: Zn2–N5 = 2.0855(14), Zn2–N6 = 2.0791(13), Zn2–N7 = 2.0927(13), Zn2–N8 = 2.0989(14), Zn2–O9 = 2.2594(16), S3–S4 = 2.0388(6) Å; N5–Zn2–N6 = 80.05(5), N5–Zn2–N7 = 158.67(6), N6–Zn2–N7 = 116.70(5), N5–Zn2–N8 = 94.17(6), N6–Zn2–N8 = 146.32(6), N7–Zn2–N8 = 78.89(5), N5–Zn2–O9 = 84.27(6), N6–Zn2–O9 = 89.99(5), N7–Zn2–O9 = 82.72(5), N8–Zn2–O9 = 122.67(5)°. (b) Space-filling diagram of the same $[Zn(\mathbf{4})(OClO_4)][ClO_4]$ unit shown in (a); the lower perchlorate ion contains O1 and is bound to the zinc ion.

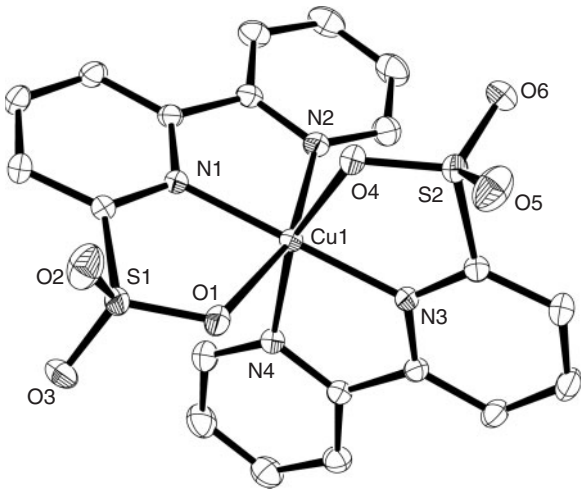

Fig. 7. Structure of the $[Cu(\mathbf{5})_2]$ molecule in $[Cu(\mathbf{5})_2]\cdot 2.5MeCN$; H atoms are omitted. Ellipsoids are plotted at the 40% probability level. Selected bond parameters: Cu1–N1 = 1.9635(13), Cu1–N2 = 2.1276(17), Cu1–N3 = 1.9620(13), Cu1–N4 = 2.1155(15), Cu1–O4 = 2.2215(13), Cu1–O1 = 2.2444(15), S1–O2 = 1.4385(15), S1–O3 = 1.4452(14), S1–O1 = 1.4650(12), S1–C1 = 1.7893(18), S2–O5 = 1.4363(15), S2–O6 = 1.4443(15), S2–O4 = 1.4670(12), S2–C11 = 1.7914(17) Å; N1–Cu1–O1 = 80.93(6), N1–Cu1–N2 = 79.23(7), N3–Cu1–O4 = 80.99(5), N3–Cu1–N4 = 79.37(6), O4–Cu1–O1 = 85.47(5)°.

domains (separation between least-squares planes = 3.31 Å), and further π-stacking involving the other bpy unit in the complex (separation between least-squares planes = 3.35 Å) results in the propagation of chains (Fig. 8). All chains run parallel to one another through the crystal lattice, with $CH_{pyridine}\cdots O_{sulfonate}$ hydrogen bonds operating between adjacent chains. Acetonitrile molecules occupy cavities between the chains. One MeCN molecule is ordered, but the remaining 1.5 solvent molecules are disordered and have been modelled over four positions.

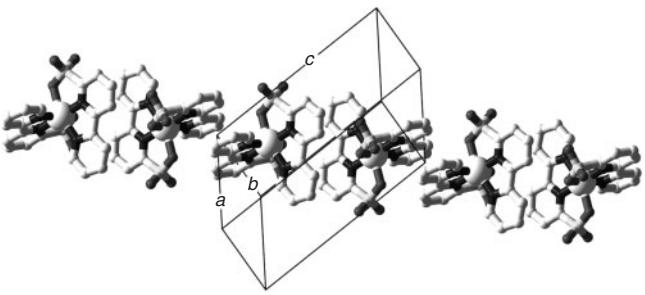

Fig. 8. Part of one chain of $[Cu(\mathbf{5})_2]$ molecules in $[Cu(\mathbf{5})_2]\cdot 2.5MeCN$, assembled through π-stacking of bpy domains. Hydrogen atoms are omitted.

Not surprisingly, the isolation of copper(I) complexes containing **4** proved difficult, and we therefore turned our attention to using the known stability of the $\{Cu^{II}(bpy)(tpy)\}$ motif.[1,2] We have previously reported the synthesis of the 2,2′:6′,2″-terpyridyl analogue of disulfide **4**, ligand **6** (Scheme 1) and of the related bis(2,2′:6′,2″-terpyridin-6-yl)disulfide, and their coordination behaviour towards iron(II) and ruthenium(II).[15,16] We argued that, in the presence of a mixture of ligands **4** and **6**, copper(II) would show a preference for a $\{Cu(bpy)(tpy)\}$ coordination environment over either $\{Cu(bpy)_2\}$ or $\{Cu(tpy)_2\}$. Equimolar amounts of $Cu(ClO_4)_2\cdot 6H_2O$, **4** and **6** were heated under microwave conditions. After workup, a solid blue product was isolated, but attempts to purify the bulk sample were not successful. However, X-ray-quality blue blocks grew after slow diffusion of Et_2O into a $MeNO_2$/MeOH solution of the crude product. The highest mass peak envelope in the electrospray mass spectrum of a MeCN solution of the crystals appeared at *m/z* 1327.0 and was assigned to $[Cu_2(\mathbf{4})(\mathbf{6})(ClO_4)_3]^+$; the

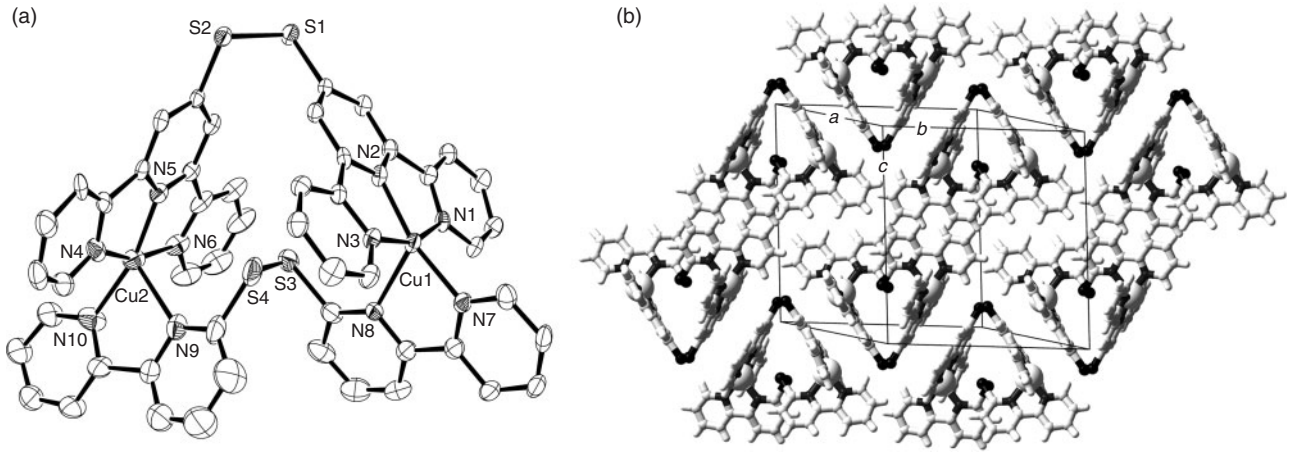

Fig. 9. (a) Structure of the $[Cu_2(\mu\text{-}\mathbf{4})(\mu\text{-}\mathbf{6})]^{4+}$ cation in $2\{[Cu_2(\mu\text{-}\mathbf{4})(\mu\text{-}\mathbf{6})][ClO_4]_4\}\cdot 5MeNO_2\cdot 2MeOH\cdot 6H_2O$ (ellipsoids plotted at 40% probability level, and H atoms omitted). The pyridine ring containing atom N10 is disordered (see text), and only one position is shown. Selected bond parameters: Cu1–N1 = 2.030(6), Cu1–N2 = 1.931(6), Cu1–N3 = 2.028(6), Cu1–N7 = 2.002(6), Cu1–N8 = 2.252(6), Cu2–N4 = 2.042(7), Cu2–N5 = 1.928(6), Cu2–N6 = 2.024(7), Cu2–N9 = 2.261(7), Cu2–N10 = 2.013(15), S1–S2 = 2.036(2), S3–S4 = 2.037(5) Å; N1–Cu1–N2 = 79.6(2), N2–Cu1–N3 = 80.6(2), N2–Cu1–N7 = 166.0(3), N2–Cu1–N8 = 117.0(2), N7–Cu1–N8 = 76.9(2), N4–Cu2–N5 = 79.7(3), N5–Cu2–N6 = 80.2(2), N5–Cu2–N9 = 116.0(2), N5–Cu2–N10 = 166.2(5), N9–Cu2–N10 = 76.1(4)°. (b) Packing of $[Cu_2(\mu\text{-}\mathbf{4})(\mu\text{-}\mathbf{6})]^{4+}$ cations; N and S atoms are shown in black.

calculated isotope distribution was consistent with this formulation. Lower mass peak envelopes at *m/z* 1066.2, 690.1 (base peak), and 536.0 were assigned to the ions $[Cu(\mathbf{4})(\mathbf{6})(ClO_4)]^+$, $[Cu(\mathbf{6})(ClO_4)]^+$, and $[Cu(\mathbf{4})(ClO_4)]^+$. Significantly, the second most intense peak (40% abundance) in the electrospray ionization (ESI) mass spectrum came at *m/z* 613.1 and was consistent with $[Cu(\mathbf{7})(ClO_4)]^+$, and is evidence for the cleavage and recombination reaction shown in Scheme 2.[18]

Single-crystal X-ray analysis of the blue crystals confirmed the formation of $[Cu_2(\mu\text{-}\mathbf{4})(\mu\text{-}\mathbf{6})][ClO_4]_4$, isolated as $[Cu_2(\mu\text{-}\mathbf{4})(\mu\text{-}\mathbf{6})][ClO_4]_4\cdot 2MeNO_2\cdot MeOH\cdot 3H_2O$. Although the structure is of poor quality, it unambiguously confirms the presence of the $[Cu_2(\mu\text{-}\mathbf{4})(\mu\text{-}\mathbf{6})]^{4+}$ cation with each copper(II) ion in a five-coordinate {Cu(bpy)(tpy)} environment (Fig. 9a). Each Cu atom exhibits a weak contact to an O atom of a perchlorate ion (Cu1···O1 = 2.815(5), Cu2···O5 = 2.764(8) Å) that fills the otherwise vacant position (see Fig. 9a) in the coordination sphere of each copper(II) centre. The pyridine ring shown in Fig. 9a to contain atom N10 is disordered and has been modelled over two equal occupancy sites. This disorder makes a detailed analysis of the coordination sphere of Cu2 meaningless. However, we note that the two tpy domains of ligand **6** bend in towards one another, generating a V-shaped cavity that accommodates the disulfide bridge of ligand **4**. The cations pack in an interdigitated assembly of rows that follow the direction of the *b*-axis (Fig. 9b). Although the diagram in Fig. 9b suggests that the tpy domains might be π-stacked, they are slipped with respect to one another and despite an inter-ring separation of 3.2 Å, the face-to-face interactions are inefficient. Better overlap is prevented by the presence of the perchlorate ions, which sit over the copper atoms (see above). All perchlorate ions are ordered, but there is significant disorder among the solvent molecules.

Conclusions

We have shown that 1,2-bis(2,2′-bipyridin-6-yl)disulfide **4** can by produced by the oxidative coupling of 6-(pyridin-2-yl)pyridine-2(1*H*)-thione **3**, using H_2O_2 as oxidant. Ligand **4** acts as a bis(chelate) to a single zinc(II) centre, giving a helical coordination environment that is completed by one *O*-bonded perchlorate ion. The same coordination motif is observed when a methyl substituent is introduced into the 6′-position of **4** (to give ligand **2**) and the pitch of the single-strand helix changes from 35.59(12)° and 37.27(12)° in the two independent $[Zn(\mathbf{4})(OClO_3)]^+$ cations to 51.3(5)° in $[Zn(\mathbf{2})(OClO_3)]^+$. The reaction of **4** with $[Cu(NCMe)_4][PF_6]$ leads to a product, tentatively formulated as $\{[Cu(\mathbf{4})][PF_6]\}_n$, aerial oxidation of which gives the octahedral copper(II) complex $[Cu(\mathbf{5})_2]$ (H**5** = 2,2′-bipyridine-6-sulfonic acid) in which $[\mathbf{5}]^-$ acts as an *N*,*N*′,*O*-donor. By applying a strategy that utilizes the preference shown by copper(II) for a five-coordinate {Cu(bpy)(tpy)} environment, we have shown that copper(II) reacts with a 1:1 mixture of **4** and **6** to produce $[Cu_2(\mu\text{-}\mathbf{4})(\mu\text{-}\mathbf{6})]^{4+}$, isolated and structurally characterized as the perchlorate salt.

Experimental

General

Room-temperature ^1H and ^{13}C NMR spectra were recorded on a Bruker Avance DPX 500 spectrometer; Scheme 1 gives the numbering scheme for **3** and **4**. Chemical shifts for ^1H and ^{13}C NMR spectra are referenced to residual solvent peaks (TMS = δ 0 ppm). MALDI-time of flight and electrospray mass spectra were recorded using PerSeptive Biosystems Voyager and MAT LCQ mass spectrometers respectively. Microwave reactions were carried out in a Biotage Initiator 8 reactor.

Caution! Perchlorate salts are potentially explosive and must be handled with caution.

6-(Pyridin-2-yl)pyridine-2(1H)-thione **3**

Compound **3** was prepared by an analogous route to that reported,[14] but starting with 6-chloro-2,2′-bipyridine (0.598 g, 3.14 mmol) in place of 6-bromo-2,2′-bipyridine. Compound **3** was isolated as a yellow solid, which was recrystallized from ethyl acetate and hexanes (0.355 g, 60%). Mp 118°C. ^1H NMR (500 MHz, $CDCl_3$ with dithiothreitol[26] added) δ/ppm 8.67 (br d, $J \approx 4.0$, 1H, H^{A6}),7.83 (m, 2H, H^{A4+A3}), 7.53 (d, J 8.6, H^{B5}), 7.41 (m, 1H, H^{A5}), 7.36 (t, J 7.9, 1H, H^{B4}), 7.18 (d, J 7.1, 1H, H^{B3}). ^{13}C NMR (126 MHz, $CDCl_3$) δ/ppm 179.5 (C^{B6}), 149.6 (C^{A6}), 146.5 (C^{A2}), 143.8 (C^{B2}), 137.9 (C^{A4}), 136.9 (C^{B4}), 134.7

(C^{B5}), 125.6 (C^{A5}), 120.0 (C^{A3}), 109.5 (C^{B3}). *m/z* (ESI-MS; MeOH) 211.3 $[M + Na]^+$ (base peak), 189.2 $[M + H]^+$.

1,2-Bis(2,2′-bipyridin-6-yl)disulfide ***4***

Compound **3** (84.5 mg, 0.449 mmol) was dissolved in MeCN (~10 mL), and H_2O_2 (30%, 0.25 mL) was added dropwise. The reaction mixture was stirred vigorously at room temperature for 2 h, and was then left in the refrigerator overnight. The colourless crystalline product **4** was separated by filtration (71.3 mg, 85%). Mp 123°C. ^{1}H NMR (500 MHz, $CDCl_3$) δ/ppm 8.64 (br d, J ~4.0, 1H, H^{A6}), 8.34 (d, J 7.9, 1H, H^{A3}), 8.20 (d, J 7.1, 1H, H^{B3}), 7.72 (m, 2H, H^{A4+B4}), 7.65 (d, J 7.9, 1H, H^{B5}), 7.27 (m, 1H, H^{A5}). ^{13}C NMR (126 MHz, $CDCl_3$) δ/ppm 158.6 (C^{B6}), 156.4 (C^{B2}), 155.4 (C^{A2}), 149.4 (C^{A6}), 138.4 ($C^{A4/B4}$), 137.2 ($C^{A4/B4}$), 124.3 (C^{A5}), 121.6 (C^{A3}), 120.0 (C^{B5}), 118.5 (C^{B3}). *m/z* (ESI-MS; MeOH) 397.3 $[M + Na]^+$ (base peak), 375.3 $[M + H]^+$. Anal. calc. for $C_{20}H_{14}N_4S_2$ (374.48) C 64.15, H 3.77, N 14.96. Found: C 63.67, H 3.94, N 15.00%.

*[Zn(**2**)$_2$][ClO$_4$]$_2$*

Compound **2** (26.5 mg, 0.0658 mmol) was suspended in MeCN (10 mL) and $Zn(ClO_4)_2 \cdot 6H_2O$ (24.5 mg, 0.0658 mmol) was added while the colourless reaction mixture was stirred. After being heated at reflux for 1 h, the reaction mixture was allowed to cool to room temperature. It was concentrated to ~one-third of the volume and then Et_2O was diffused into the solution overnight. The colourless precipitate was separated by filtration and dried under high vacuum to yield $[Zn(\mathbf{2})_2][ClO_4]_2$ as an off-white microcrystalline solid (33.8 mg, 77.0%). ^{1}H NMR (500 MHz, CD_3CN) δ/ppm 8.61 (d, J 8.1, 1H, H^{B3}), 8.47 (d, J 8.0, 1H, H^{A3}), 8.37 (t, J 7.9, 1H, H^{B4}), 8.29 (t, J 7.9, 1H, H^{A4}), 8.12 (d, J 7.8, 1H, H^{B5}), 7.67 (d, J 7.8, 1H, H^{A5}), 1.99 (s, 3H, H^{Me}). ^{13}C NMR (126 MHz, CD_3CN) δ/ppm 160.4 (C^{A6}), 158.9 (C^{B6}), 153.5 (C^{B2}), 148.6 (C^{A2}), 144.5 (C^{B4}), 143.6 (C^{A4}), 132.2 (C^{B5}), 130.7 (C^{A5}), 124.4 (C^{B3}), 122.8 (C^{A3}), 24.1 (C^{Me}). *m/z* (MALDI MS) 466.53 $[Zn(\mathbf{2})]^+$. Anal. calc. for $C_{22}H_{18}Cl_2N_4O_8S_2Zn$ (666.85) C 39.63, H 2.72, N 8.40. Found C 39.64, H 2.88, N 8.67%.

*[Zn(**4**)$_2$][ClO$_4$]$_2$*

Compound **4** (21.9 mg, 0.0585 mmol) was suspended in MeCN (10 mL) and $Zn(ClO_4)_2 \cdot 6H_2O$ (21.8 mg, 0.0585 mmol) was added to the stirring mixture. After being heated at reflux for 1 h, the reaction mixture was allowed to cool to room temperature, and was concentrated to ~one-third of its volume. Slow diffusion of Et_2O into the solution overnight yielded a colourless precipitate, which was separated by filtration and dried under high vacuum. $[Zn(\mathbf{4})_2][ClO_4]_2$ was isolated as an off-white microcrystalline solid (31.6 mg, 84.6%). ^{1}H NMR (500 MHz, CD_3CN) δ/ppm 8.57 (m, 2H, H^{A3+B3}), 8.41 (t, J 7.8, 1H, H^{A4}), 8.37 (d, J 4.9, 1H, H^{A6}), 8.32 (t, J 7.9, 1H, H^{B4}), 8.06 (d, J 7.8, 1H, H^{B5}), 7.85 (m, 1H, H^{A5}). ^{13}C NMR (126 MHz, CD_3CN) δ/ppm 159.0 (C^{B6}), 153.0 (C^{B2}), 149.8 (C^{A6}), 149.3 (C^{A2}), 144.2 (C^{B4}), 143.8 (C^{A4}), 131.3 (C^{B5}), 129.2 (C^{A5}), 124.7 ($C^{A3/B3}$), 124.1 ($C^{A3/B3}$). *m/z* (MALDI MS) 538.57 $[Zn(\mathbf{4})ClO_4]^+$. Anal. calc. for $C_{20}H_{14}Cl_2N_4O_8S_2Zn$ (638.79) C 37.61, H 2.21, N 8.77. Found C 37.58, H 2.27, N 8.90%.

*[Cu(**5**)$_2$]·2.5MeCN*

Compound **4** (28.1 mg, 0.075 mmol) was suspended in MeCN and the mixture degassed with N_2 for 15 min. $[Cu(NCMe)_4][PF_6]$ (28.0 mg, 0.075 mmol) was added while the mixture was stirred, causing an immediate colour change to dark red-brown. The reaction mixture was heated at reflux for 1 h and allowed to cool to room temperature. The solution was concentrated to one-third of its volume, and then Et_2O was allowed to diffuse into it over a period of 2 days. A red-orange precipitate was collected by filtration. Attempts to isolate a pure sample of the product were unsuccessful. ^{1}H NMR (400 MHz, CD_3CN) δ/ppm 8.50 (br, 1H), 8.28 (br, 1H), 8.16 (br, 1H), 8.02 (br, 1H), 7.81 (br, 1H), 7.60–7.54 (br, overlapping, 2H). After several months, green crystals of $[Cu(\mathbf{5})_2]\cdot 2.5MeCN$ had formed in the NMR tube.

*[Cu$_2$(μ-**4**)(μ-**6**)][ClO$_4$]$_4$*

Compounds **4** (9.2 mg, 0.0245 mmol) and **6** (13.0 mg, 0.0245 mmol) were suspended in MeCN (2 mL) and $Cu(ClO_4)_2 \cdot 6H_2O$ was added (18.2 mg, 0.0491 mmol). The reaction mixture was sealed in a vial and heated in a microwave reactor at 120°C for 10 min, then allowed to cool to room temperature. The solid product was separated by filtration. A sample of the crude product was dissolved in $MeNO_2$ with a drop of MeOH added, and Et_2O was allowed to diffuse into the solution. Crystals of $[Cu_2(\mu\text{-}\mathbf{4})(\mu\text{-}\mathbf{6})][ClO_4]_4 \cdot 2MeNO_2 \cdot MeOH \cdot 3H_2O$ formed overnight. *m/z* (ESI MS; MeCN) 1327.0 $[Cu_2(\mathbf{4})(\mathbf{6})(ClO_4)_3]^+$, 1066.2 $[Cu(\mathbf{4})(\mathbf{6})(ClO_4)]^+$, 690.1 $[Cu(\mathbf{6})(ClO_4)]^+$ (base peak), 536.0 $[Cu(\mathbf{4})(ClO_4)]^+$ (see text).

Crystal Structure Determinations

Data were collected on Bruker-Nonius Kappa charge coupled device or Stoe IPDS diffractometers; data reduction, solution and refinement used the programs *COLLECT*,[30] *SIR92*,[31] *DENZO/SCALEPACK*,[32] and *CRYSTALS*,[33] or Stoe *IPDS* software[34] and *SHELXL97*.[35] Hydrogen atoms bonded to N or O have been located, optimized, and then included as fixed contributions. *ORTEP* figures were drawn with the program *ORTEP-3* for Windows.[36] Structures were analyzed using *Mercury* v. 2.3.[37,38]

3: $C_{10}H_8N_2S$, M 188.25, colourless plate, triclinic, space group $P\bar{1}$, a 7.9706(1), b 9.5618(2), c 12.1532(2) Å, α 77.4044(9), β 76.2747(9), γ 87.3699(10)°, U 878.11(3) Å^3, Z 4, D 1.424 Mg m^{-3}, μ(MoKα) 0.315 mm^{-1}, F(000) 392, T 173 K, 10187 reflections, 5146 unique (R_{int} 0.025), R_1 0.0358 (3131 reflections, 235 parameters, $I > 3.0\sigma(I)$), wR_2 0.0458, R_1 0.0647 (all data), wR_2 0.0564 (all data), goodness of fit (GOF) 1.0221.

4: $C_{20}H_{14}N_4S_2$, M 374.49, colourless block, monoclinic, space group $C2/c$, a 19.253(4), b 7.9777(16), c 11.636(2) Å, β 105.62(3)°, U 1721.2(6) Å^3, Z 4, D 1.445 Mg m^{-3}, μ(MoKα) 0.321 mm^{-1}, F(000) 776, T 173 K, 21632 reflections, 3124 unique (R_{int} 0.0364), R_1 0.0385 (3009 reflections, 118 parameters, $I > 2.0\sigma(I)$), wR_2 0.1067, R_1 0.0400 (all data), wR_2 0.1078 (all data), GOF 1.101.

2{[Zn(**2**)(OClO$_3$)][ClO$_4$]}·EtOH: $C_{46}H_{42}Cl_4N_8O_{17}S_4Zn_2$, M 1379.72, colourless plate, monoclinic, space group $C2/c$, a 28.5683(12), b 10.4110(5), c 22.0368(10) Å, β 125.360(2)°, U 5345.3(4) Å^3, Z 4, D 1.714 Mg m^{-3}, μ(MoKα) 1.334 mm^{-1}, F(000) 2808, T 173 K, 33248 reflections, 5209 unique (R_{int} 0.066), R_1 0.0728 (3791 reflections, 377 parameters, $I > 1.0\sigma(I)$), wR_2 0.0798, R_1 0.1000 (all data), wR_2 0.1029 (all data), GOF 1.1410.

[Zn(**4**)(OClO$_3$)][ClO$_4$]: $C_{20}H_{14}Cl_2N_4O_8S_2Zn$, M 638.77, colourless block, monoclinic, space group $P2_1/c$, a 15.2359(8), b 16.2519(9), c 19.4989(11) Å, β 109.732(3)°, U 4544.7(4) Å^3,

Z 8, D 1.867 Mg m^{-3}, μ(MoKα) 1.559 mm^{-1}, F(000) 2576, T 123 K, 117679 reflections, 17252 unique (R_{int} 0.035), R_1 0.0436 (14030 reflections, 667 parameters, $I > 2.0\sigma(I)$), wR_2 0.0459, R_1 0.0481 (all data), wR_2 0.0615 (all data), GOF 1.0630.

[Cu(**5**)$_2$]·2.5MeCN: $C_{25}H_{21.5}CuN_{6.5}O_6S_2$, M 636.65, green block, triclinic, space group $P\bar{1}$, a 11.0071(14), b 11.0069(13), c 14.3152(16) Å, α 96.414(10), β 105.283(9), γ 117.951(9)°, U 1420.4(3) Å^3, Z 2, D 1.489 Mg m^{-3}, μ(MoKα) 0.967 mm^{-1}, F(000) 652, T 173 K, 70149 reflections, 8152 unique (R_{int} 0.1101), R_1 0.0359 (8024 reflections, 438 parameters, $I > 2.0\sigma(I)$), wR_2 0.1039, R_1 0.0363 (all data), wR_2 0.1043 (all data), GOF 1.065.

[Cu$_2$(μ-**4**)(μ-**6**)][ClO$_4$]$_4$·2MeNO$_2$·MeOH·3H$_2$O: $C_{53}H_{50}Cl_4Cu_2N_{12}O_{24}S_4$, M 1636.21, blue block, triclinic, space group $P\bar{1}$, a 14.5596(11), b 16.0545(13), c 17.5368(14) Å, α 91.668(5), β 111.507(4), γ 109.858(4)°, U 3531.3(5) Å^3, Z 2, D 1.539 Mg m^{-3}, μ(MoKα) 0.955 mm^{-1}, F(000) 1648, T 123 K, 43521 reflections, 16286 unique (R_{int} 0.067), R_1 0.1048 (8553 reflections, 1018 parameters, $I > 2.0\sigma(I)$), wR_2 0.0987, R_1 0.1773 (all data), wR_2 0.1530 (all data), GOF 1.0804.

The crystal data have been deposited with the Cambridge Crystallographic Data Centre (www.ccdc.cam.ac.uk; nos. CCDC 767120–767125).

Acknowledgements

We thank the Swiss National Science Foundation and the University of Basel for financial support.

References

[1] V. Chaurin, E. C. Constable, C. E. Housecroft, *New J. Chem.* **2006**, *30*, 1740. doi:10.1039/B610306E

[2] E. C. Constable, S. Decurtins, C. E. Housecroft, T. D. Keene, C. G. Palivan, J. R. Price, J. A. Zampese, *Dalton Trans.* **2010**, *39*, 2337. doi:10.1039/B923729A

[3] E. C. Constable, C. E. Housecroft, M. Neuburger, J. R. Price, J. A. Zampese, *CrystEngComm* **2010**, in press. doi:10.1039/C002827D

[4] A. Albert, G. B. Barlin, *J. Chem. Soc.* **1959**, 2384.

[5] S. Stoyanov, I. Petkov, L. Antonov, T. Stoyanova, P. Karagiannidis, P. Aslanidis, *Can. J. Chem.* **1990**, *68*, 1482. doi:10.1139/V90-227

[6] P. Beak, F. S. Fry, Jr, J. Lee, F. Steele, *J. Am. Chem. Soc.* **1976**, *98*, 171. doi:10.1021/JA00417A027

[7] M. J. Cook, S. El-Abbady, A. R. Katritzky, C. Guimon, G. Pfister-Guillouzo, *J. Chem. Soc., Perkin Trans. 2* **1977**, 1652.

[8] M. Hunziker, U. Hauser, *Heterocycles* **1982**, *19*, 2131. doi:10.3987/R-1982-11-2131

[9] A. P. Krapcho, S. Sparapani, A. Leenstra, J. D. Seitz, *Tetrahedron Lett.* **2009**, *50*, 3195. doi:10.1016/J.TETLET.2009.01.138

[10] A. P. Krapcho, S. Sparapani, M. Boxer, *Tetrahedron Lett.* **2007**, *48*, 5593. doi:10.1016/J.TETLET.2007.06.043

[11] D. Branowska, A. Rykowski, W. Wysocki, *Tetrahedron Lett.* **2005**, *46*, 6223. doi:10.1016/J.TETLET.2005.07.062

[12] P. Pornsuriyasak, N. P. Rath, A. V. Demchenko, *Chem. Commun.* **2008**, 5633.

[13] J.-P. Griffiths, R. J. Brown, P. Day, C. J. Matthews, B. Vital, J. D. Wallis, *Tetrahedron Lett.* **2003**, *44*, 3127. doi:10.1016/S0040-4039(03)00539-2

[14] Q. Wang, P. Day, J.-P. Griffiths, H. Nie, J. D. Wallis, *New J. Chem.* **2006**, *30*, 1790. doi:10.1039/B606715H

[15] E. C. Constable, B. A. Hermann, C. E. Housecroft, M. Neuburger, S. Schaffner, *New J. Chem.* **2005**, *29*, 1475. doi:10.1039/B510792J

[16] E. C. Constable, C. E. Housecroft, M. Neuburger, J. R. Price, S. Schaffner, *Dalton Trans.* **2008**, 3795.

[17] F. Wang, A. W. Schwabacher, *Tetrahedron Lett.* **1999**, *40*, 4779. doi:10.1016/S0040-4039(99)00885-0

[18] S. Otto, R. L. E. Furlan, J. K. M. Sanders, *J. Am. Chem. Soc.* **2000**, *122*, 12063. doi:10.1021/JA005507O

[19] R. J. Sarma, S. Otto, J. R. Nitschke, *Chem. Eur. J.* **2007**, *13*, 9542. doi:10.1002/CHEM.200701228

[20] M. T. Räisänen, N. Runeberg, M. Klinga, M. Nieger, M. Bolte, P. Pyykkö, M. Leskelä, T. Repo, *Inorg. Chem.* **2007**, *46*, 9954. doi:10.1021/IC700453T

[21] J. Zhang, J.-K. Cheng, Y.-Y. Qin, Z.-J. Li, Y.-G. Yao, *Inorg. Chem. Commun.* **2008**, *11*, 164. doi:10.1016/J.INOCHE.2007.11.011

[22] F. Li, L. Xu, B. Bi, X. Liu, L. Fan, *CrystEngComm* **2008**, *10*, 693. doi:10.1039/B800437B

[23] H. Wang, X.-Q. Guo, R. Zhing, X.-F. Hou, *J. Organomet. Chem.* **2009**, *694*, 1567. doi:10.1016/J.JORGANCHEM.2009.01.040

[24] W. W. Brandt, F. P. Dwyer, E. D. Gyarfas, *Chem. Rev.* **1954**, *54*, 959. doi:10.1021/CR60172A003

[25] A. J. Downard, G. E. Honey, P. J. Steel, *Inorg. Chem.* **1991**, *30*, 3733. doi:10.1021/IC00019A033

[26] W. W. Cleland, *Biochemistry* **1964**, *3*, 480. doi:10.1021/BI00892A002

[27] R. D. Shannon, *Acta Crystallogr. A* **1976**, *32*, 751. doi:10.1107/S0567739476001551

[28] W. W. Brandt, F. P. Dwyer, E. D. Gyarfas, *Chem. Rev.* **1954**, *54*, 959. doi:10.1021/CR60172A003

[29] S. Delgado, A. Molina-Ontoria, M. E. Medina, C. J. Pastor, R. Jiménez-Aparcio, J. L. Priego, *Inorg. Chem. Commun.* **2006**, *9*, 1289. doi:10.1016/J.INOCHE.2006.06.026

[30] *COLLECT Software* Nonius BV 1997–2001, Delft.

[31] A. Altomare, G. Cascarano, G. Giacovazzo, A. Guagliardi, M. C. Burla, G. Polidori, M. Camalli, *J. Appl. Cryst.* **1994**, *27*, 435.

[32] Z. Otwinowski, W. Minor, *Methods in Enzymology* **1997**, Vol. 276, p. 307 (Eds C. W. Carter, Jr, R. M. Sweet) (Academic Press: New York, NY).

[33] P. W. Betteridge, J. R. Carruthers, R. I. Cooper, K. Prout, D. J. Watkin, *J. Appl. Cryst.* **2003**, *36*, 1487. doi:10.1107/S0021889803021800

[34] *Stoe & Cie IPDS Software v. 1.26* **1996** (Stoe & Cie: Darmstadt).

[35] G. M. Sheldrick, *Acta Crystallogr. A* **2008**, *64*, 112. doi:10.1107/S0108767307043930

[36] L. J. Farrugia, *J. Appl. Cryst.* **1997**, *30*, 565. doi:10.1107/S0021889897003117

[37] I. J. Bruno, J. C. Cole, P. R. Edgington, M. K. Kessler, C. F. Macrae, P. McCabe, J. Pearson, R. Taylor, *Acta Crystallogr. B* **2002**, *58*, 389. doi:10.1107/S0108768102003324

[38] C. F. Macrae, I. J. Bruno, J. A. Chisholm, P. R. Edgington, P. McCabe, E. Pidcock, L. Rodriguez-Monge, R. Taylor, J. van de Streek, P. A. Wood, *J. Appl. Cryst.* **2008**, *41*, 466. doi:10.1107/S0021889807067908